Exact Inversion of the Exponential X-ray Transform for RSH SPECT

J.-M. Wagner,[1] F. Noo,[2] R. Clackdoyle[2] *

[1]University of Liège, Belgium [2]University of Utah, USA

Abstract

The RSH SPECT scanner provides parallel-beam attenuated projections for a fully 3D acquisition geometry. The geometry can be represented by circles on the unit sphere of projection directions, one circle for each position of the detector head. Unlike most other fully 3D geometries this one is particularly challenging because there are no 2D subsets in the data. When no attenuation is present, it is well-known that an unmeasured projection can be synthesized if it lies inside one of the measured circles. The main result of this work is that under some assumptions on the attenuation distribution, *attenuated* projections within a circle can be synthesized from available attenuated projections. One consequence is that RSH SPECT projections can be rebinned into a conventional SPECT geometry for which analytic attenuation correction techniques are available.

1 Introduction

In Single Photon Emission Computed Tomography (SPECT) imaging the objective is to visualize the concentration of a radioactive tracer within the 3D body under investigation. The limitations in SPECT are essentially due to attenuation of the photons and to the poor sensitivity of the collimator-detector system. A number of researchers have been considering alternatives to the conventional parallel-hole collimator (figure 1a).

The use of a rotating slant-hole (RSH) collimator with two (figure 1b) or four segments significantly increases the detection sensitivity by allowing a higher photon count during the same acquisition period [1]. The collimator-detector system is sucessively placed at different angular positions around the body to be studied. For each of these positions, the collimator is rotated about its center, while allowing several projections (two or four according to the collimator used) to be acquired simultaneously. This acquisition mode constitutes the RSH SPECT geometry as described in [1].

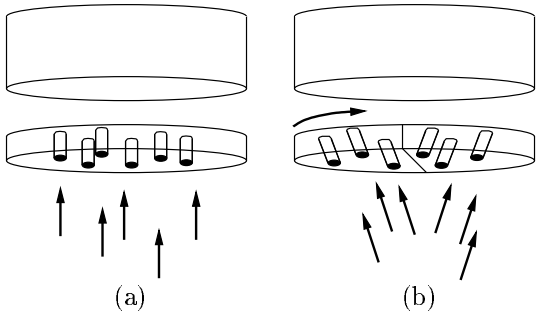

Figure 1: Different types of collimators. a) conventional parallel-hole collimator, b) RSH collimator.

The RSH SPECT scanner provides a set of attenuated projections. The exponential X-ray transform is a mathematical tool used in SPECT reconstruction for modeling and correcting for attenuation. Using the exponential X-ray transform, it is possible to reconstruct the emission map with attenuation correction, assuming the attenuation is constant in the emission region. Attenuated projections can be converted to exponential X-ray projections using a well-known point-by-point scaling [2]. Moreover, even if the attenuation map is unknown, the consistency conditions of the exponential X-ray transform provide an effective method to find the scaling coefficients [3].

In two-dimensions (2D), image reconstruction from exponential X-ray projections has been thoroughly studied over the past twenty-five years and is now well understood, especially due to the works of Tretiak & Metz [9] and Pan & Metz [10]. A very recent work [11] provides an inversion formula for the case of only 180-degrees of exponential data. The acquisition geometry for RSH SPECT is a fully 3D geometry for which an inversion formula for

*This work was partially supported by the National Institutes of Health, grant number R01 HL55610.

the X-ray transform has not yet been established. To our knowledge, only a few simple geometries have been treated. In [4] and [5], the exponential projections must be finely sampled on the unit sphere while the algorithm described in [6] only handles collections of projections on any subset of the unit sphere described as a union of great circles. Currently, we do not know if it is possible to obtain exact reconstructions from more general collections, such as those satisfying Orlov's condition [7] for the non-attenuated case.

We give a description of the general RSH geometry in section 2. In section 3, we generalize Orlov's result [7] and establish a rebinning technique which allows us to calculate new exponential projections (with any attenuation coefficient) from exponential projections given on a circle in the RSH geometry. Finally, in section 4, we use these new theoretical results to obtain a method of exact reconstruction from a set of complete exponential projections (complete in the sense of Orlov [7]) for the RSH SPECT geometry.

2 The RSH SPECT Geometry

Figure 2 illustrates the RSH SPECT geometry. In this figure, O is the origin of the unit sphere S^2. The orientation of the detector with respect to the origin is given by its unit normal vector $\underline{c}_i$. We assume N different positions of the detector ($i = 1, 2, \ldots, N$). Also, we assume that for each position i of the detector, the collimator has a slant angle equal to α_i. The unit vector $\underline{n}$ defines the direction of photon propagation through the collimator. When it effects a rotation of 360 degrees about itself, the vector $\underline{n}$ describes, on the unit sphere, a circle C_i of angular aperture α_i and whose axis of symmetry is the vector $\underline{c}_i$. The RSH SPECT geometry is mathematically defined by the trajectory Ω on the unit sphere corresponding to the union of all the circles C_i.

After conversion from attenuated projections, the data available for image reconstruction are the exponential X-ray projections

$$p_\mu(\underline{n}, \underline{s}) = \int_{-\infty}^{+\infty} dt\, f(\underline{s} + t\underline{n})\, e^{-\mu t}, \qquad \underline{s}.\underline{n} = 0 \qquad (1)$$

for the directions $\underline{n} \in \Omega$. The 3D image to reconstruct is f while μ is the known, constant attenuation coefficient.

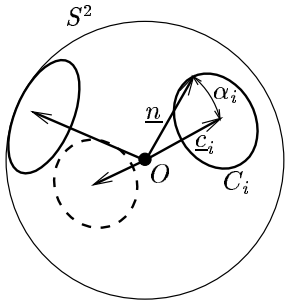

Figure 2: Illustration of the RSH SPECT geometry.

3 Theory

We show here that it is possible to calculate any parallel projection (with any finite attenuation coefficient μ_1) of whose direction $\underline{\alpha}$ is situated in the region of the unit sphere bounded by one of the circles making up Ω. In section 4 we show how the rebinning technique can be used to create, from the RSH SPECT data, a collection of exponential projections corresponding to a conventional parallel-hole SPECT geometry for which an exact inversion formula exists. An example reconstruction is given.

Let us consider one of the circles C_i making up Ω and let $\underline{\alpha}$ be a unit vector situated in the region of S^2 bounded by C_i. Figure 3 illustrates the situation. We use $\mathcal{C}(\underline{\alpha})$ to denote the great circle orthogonal to $\underline{\alpha}$ and we introduce four unit vectors $\underline{a}$, $\underline{b}$, $\underline{\theta}$ and $\underline{\theta}^\perp$ all lying on the great circle $\mathcal{C}(\underline{\alpha})$. The vectors $\underline{a}$ and $\underline{b}$ are defined mathematically by

$$\underline{a} = \frac{\underline{c}_i \times \underline{\alpha}}{||\underline{c}_i \times \underline{\alpha}||}, \quad \underline{b} = \underline{a} \times \underline{\alpha} \qquad (2)$$

while

$$\begin{cases} \underline{\theta} &= \cos\theta\, \underline{a} + \sin\theta\, \underline{b} \\ \underline{\theta}^\perp &= -\sin\theta\, \underline{a} + \cos\theta\, \underline{b} \end{cases} \qquad (3)$$

where θ belongs to the interval $[0, 2\pi]$. For the case where the vector $\underline{\alpha}$ corresponds to $\underline{c}_i$ we choose $\underline{a}$ arbitrarily on $\mathcal{C}(\underline{\alpha})$.

The great circle orthogonal to $\underline{\theta}$, denoted $\mathcal{C}(\underline{\theta})$, cuts the circle C_i at a point $\underline{n}$ given by

$$\underline{n} = \cos\psi(\theta)\, \underline{\alpha} + \sin\psi(\theta)\, \underline{\theta}^\perp \qquad (4)$$

where $\psi(\theta) \in]0, \pi[$ for all $\theta \in [0, 2\pi[$. We show that the function $\psi(\theta)$ is given by

$$\tan\frac{\psi(\theta)}{2} = \frac{-\sin(k\alpha_i)\, \cos\theta + \sqrt{\sin^2\alpha_i - \sin^2(k\alpha_i)\, \sin^2\theta}}{\cos\alpha_i + \cos(k\alpha_i)} \qquad (5)$$

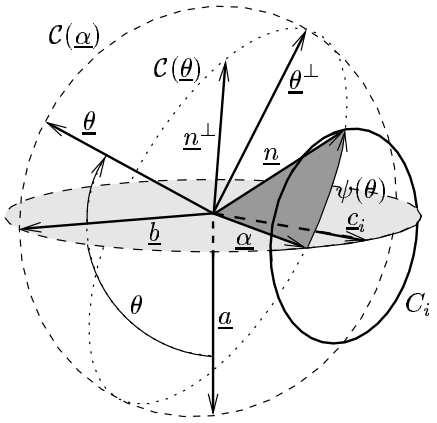

Figure 3: Rebinning from a set of exponential projections corresponding to a circle C_i.

where $(k\alpha_i)$ is the angle between $\underline{c}_i$ and $\underline{\alpha}$ ($k \in [0,1[$). Finally, we introduce the vector $\underline{n}^{\perp} = \underline{\theta} \times \underline{n} = -\sin\psi(\theta)\,\underline{\alpha} + \cos\psi(\theta)\,\underline{\theta}^{\perp}$.

From exponential projections $p_{\mu}(\underline{n},\underline{s})$ known for $\underline{n} \in C_i$, it is possible to calculate the exponential projection $p_{\mu_1}(\underline{\alpha},\underline{s})$ for any finite value μ_1 of the attenuation coefficient. To this end we show that

$$\int_{-\infty}^{+\infty} p_{\mu_1}(\underline{\alpha}, l\underline{\theta}+s\underline{\theta}^{\perp}) e^{-\mu_2(\theta)s} ds = \int_{-\infty}^{+\infty} p_{\mu}(\underline{n}, l\underline{\theta}+t\underline{n}^{\perp}) e^{-\mu_d(\theta)t} dt \tag{6}$$

where

$$\mu_2(\theta) = \frac{\mu - \mu_1 \cos\psi(\theta)}{\sin\psi(\theta)} \quad \text{and} \quad \mu_d(\theta) = \frac{\mu \cos\psi(\theta) - \mu_1}{\sin\psi(\theta)} \tag{7}$$

for all $(\theta, l) \in [0, 2\pi[\times]-\infty, +\infty[$. The expression on the left of (6) is the 2D exponential Radon transform (with attenuation μ_2 depending on projection angle, and which we will denote AD-ERT for Angle Dependent Exponential Radon Transform) of the projection $p_{\mu_1}(\underline{\alpha},\underline{s})$ while the expression on the right constitutes a sample of the 2D exponential Radon transform (with attenuation μ_d depending on angle) of the projection $p_{\mu}(\underline{n},\underline{s})$. A sample of the AD-ERT of the projection $p_{\mu_1}(\underline{\alpha},\underline{s})$ is therefore obtained by judiciously integrating in the plane of one of the available projections. By applying the relation (6) for all (θ, l), we obtain the AD-ERT of the projection $p_{\mu_1}(\underline{\alpha},\underline{s})$, which we denote $g(\theta, l)$. The problem of the inversion of the AD-ERT was resolved in [8], and allows us to reconstruct $p_{\mu_1}(\underline{\alpha},\underline{s})$ from $g(\theta, l)$:

$$p_{\mu_1}(\underline{\alpha},\underline{s}) = \int_0^{2\pi} d\theta\, g^F(\theta, \underline{s}.\underline{\theta})\, e^{\mu_2(\theta)\underline{s}.\underline{\theta}^{\perp}} \tag{8}$$

where $g^F(\theta, l)$ is given in the Fourier domain by $G^F(\theta,\sigma) = G(\theta,\sigma)\,H(\theta,\sigma)$ and

$$H(\theta,\sigma) = \begin{cases} |\sigma| - j\,\mathrm{sgn}(\sigma)\,\mu_2'(\theta) & \text{if } |\sigma| > |\mu_2(\theta)|/(2\pi) \\ 0 & \text{otherwise} \end{cases} \tag{9}$$

where $\mu_2'(\theta)$ is the derivative of $\mu_2(\theta)$ and $j = \sqrt{-1}$.

We note that although any value of μ_1 can be used in principle, it is safer in practice to use $\mu_1 = \mu$ to control the behavior of $\mu_2(\theta)$.

4 Simulations and Results

In this section, we study an example RSH SPECT geometry. The set Ω under consideration consists of 3 circles whose centers $\underline{c}_i$ are situated on the great circle $\mathcal{C}(\underline{e}_z)$ at regular intervals of 60 degrees and with a slant angle of 30 degrees (for $i = 1, 2, 3$). Figure 4 illustrates the situation. According to Orlov [7], this set is complete because all great circles on the unit sphere intersect Ω. An exact reconstruction is therefore possible in the non-attenuated case. We show below that exact reconstruction is also possible for the attenuated case.

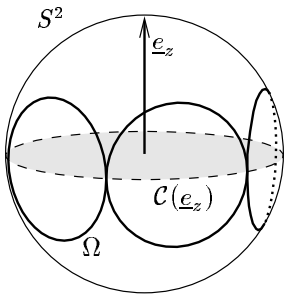

Figure 4: An example RSH SPECT geometry.

There are 3 distinct positions of the detector and we have simulated 32 angular positions of the collimator rotating about its own axis, which makes a total of $3 \times 32 = 96$ simulated attenuated projections for this RSH SPECT geometry. A phantom modeling the heart was used for the emission map. It was composed of three ellipsoids, two of which modeled the ventricles with 20% of the specific activity of the myocardium. The attenuation map

was modeled with 4 ellipsoids, representing the thorax, the two lungs, and the spinal column. Figure 5 shows the emission and attenuation maps for two slices in different orientations. Each attenuated projection was sampled on a grid of 100^2 pixels of side 1.5 mm. The attenuation coefficients being constant in the emission region, we converted the attenuated projections to exponential projections with $\mu = 0.15/\text{cm}$.

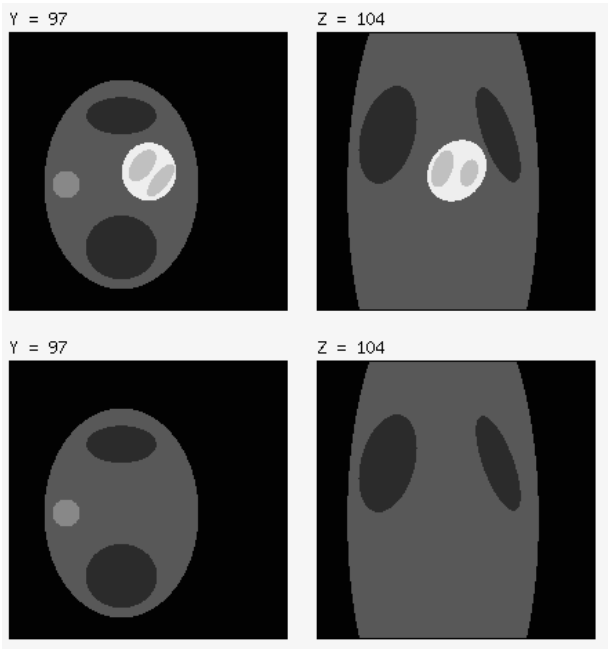

Figure 5: Top: Emission and attenuation maps superimposed. Bottom: Attenuation map only.

We applied the rebinning method (with $\mu_1 = \mu$) to calculate the exponential projections $p_\mu(\underline{\alpha}, \underline{s})$ for 181 directions $\underline{\alpha}$ uniformly sampled on the half of the great circle $\mathcal{C}(\underline{e}_z)$ with an angular step of 1 degree. The calculated projections were reconstructed on a grid of 100^2 pixels of side 1.5 mm. The details of the reconstruction algorithm will be given at the conference. Figure 6 shows one of the 181 exponential projections calculated by the rebinning method. This figure illustrates the exactness of the rebinning method.

The 181 calculated exponential projections constitute a set of projections in the conventional (180-degree) parallel-hole collimator SPECT geometry. For this configuration an exact inversion formula now exists ([11]). We have applied this algorithm to reconstruct, slice by slice perpendicular to $\underline{e}_z$, the image f on a grid of 100^3 voxels of side 1.5 mm. The quality of the reconstruction

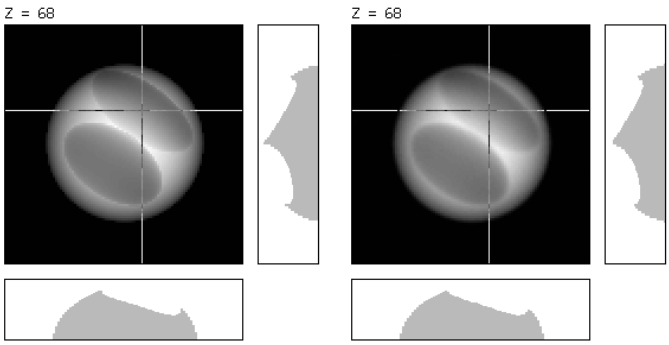

Figure 6: Illustration of the rebinning method ($k = 0.5$). Left: Ideal projection. Right: Synthesized projection.

given in figure 7 illustrates the efficacy of the reconstruction method.

Reconstructions with simulated noisy data have also been successful, and reconstructions with data from a prototype RSH SPECT scanner is being submitted to the 2001 IEEE MIC conference.

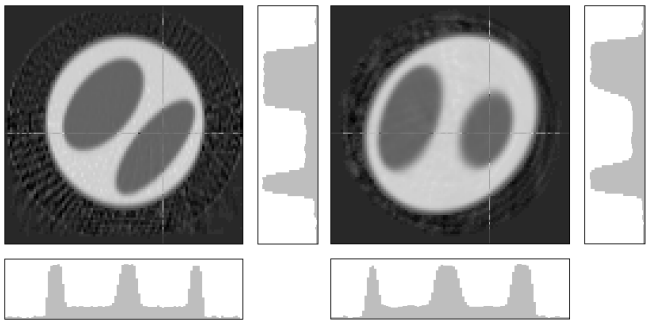

Figure 7: Heart phantom reconstruction for $\mu = 0.15/\text{cm}$.

References

[1] R. Clack, P.E. Christian, M. Defrise, A.E. Welch, "Image reconstruction for a novel SPECT system with rotating slant-hole collimators". In Conf. Rec. 1995 IEEE Med. Imag. Conf., 1948-1952, 1996.

[2] A. Markoe, "Fourier inversion of the attenuated X-ray transform", SIAM J. Math. Anal., Vol. 15(4), 718-722, 1984.

[3] C. Mennessier, F. Noo, R. Clack, G. Bal, L. Desbat, "Attenuation correction in SPECT using consistency

conditions for the exponential ray transform", Phys. Med. Biol., Vol. 44, 2483-2510, 1999.

[4] I.A. Hazou, D.C. Solmon, "Inversion of the exponential X-ray transform. I:Analysis", Math. Methods in the Applied Sciences, Vol. 10(10), 561-574 (1988).

[5] Y. Weng, G.L. Zeng, G.T. Gullberg, "Filtered backprojection algorithm for attenuated parallel and cone-beam projections sampled on a sphere", in Three-dimensional Image Reconstruction In Radiation and Nuclear Medicine, ed. P. Grangeat and J.-L. Amans (Dordrecht: Kluwer), 19-34, 1996.

[6] J.-M. Wagner, F. Noo, "TTR algorithm for the inversion of the exponential X-ray transform". In Conf. Rec. IEEE 2000 Med. Imag. Conf., to be published.

[7] S.S. Orlov, "Theory of three dimensional reconstruction. 1. Conditions of a complete set of projections.", Sov. Phys.-Crystallogr., Vol. 20, 312-314, 1975.

[8] P. Kuchment, I. Shneiberg, "Some Inversion formulas in the Single Photon Emission Computed Tomography", Appl. Anal., vol. 53, 221-231, 1994.

[9] O. Tretiak, C. Metz, "The exponential Radon transform", SIAM, J. Appl. Math., Vol. 39(2), 341-354, 1980.

[10] C.E. Metz, X. Pan, "A unified analysis of exact methods of inverting the 2D exponential Radon tranform, with implications for Noise control in SPECT", IEEE Trans. Med. Imag., vol. 14(4), 643-658, 1995.

[11] F. Noo, J.-M. Wagner, "Image reconstruction in 2D SPECT with 180-degree acquisition," submitted to Inverse Problems.